

Probability distribution of returns for a model with stochastic volatility

Adrian A. Drăgulescu* and Victor M. Yakovenko†

Department of Physics, University of Maryland, College Park, MD 20742-4111, USA

(Dated: 3 March 2002, **cond-mat/0203046**)

We study a model where stock price dynamics is governed by a geometrical (multiplicative) Brownian motion with stochastic variance. We solve the corresponding Fokker-Planck equation exactly, using either the method of characteristics or path integrals. After integrating out the variance, we find an analytic formula for the time-dependent probability distribution of stock price changes (returns). The formula is in excellent agreement with the Dow-Jones index for the time lags from 1 to 250 trading days. For large returns, the distribution is exponential in log-returns with a time-dependent exponent, whereas for small returns it is Gaussian. For time lags longer than the relaxation time of variance, the probability distribution can be expressed in a scaling form using a Bessel function. The Dow-Jones data follow the scaling function for seven orders of magnitude.

I. INTRODUCTION

Stochastic dynamics of stock prices is commonly described by a geometric (multiplicative) Brownian motion, which gives a log-normal probability distribution for stock price changes (returns) [1]. However, numerous observations show that the tails of the distribution decay slower than the log-normal distribution predicts (the so-called “fat-tails” effect) [2, 3, 4]. Particularly, much attention was devoted to the power-law tails [5, 6]. The geometric Brownian motion model has two parameters: the drift μ , which characterizes the average growth rate, and the volatility σ , which characterizes the noisiness of the process. There is empirical evidence and a set of stylized facts indicating that volatility, instead of being a constant parameter, is driven by a mean-reverting stochastic process [7, 8]. Various mathematical models with stochastic volatility have been discussed in literature [9, 10, 11, 12].

In this paper, we study a particular stochastic volatility model, where the square root of the stock-price volatility, called the variance, follows a random process known in financial literature as the Cox-Ingersoll-Ross process and in mathematical statistics as the Feller process [8, 11]. We solve the Fokker-Planck equation for this model exactly and find the joint probability distribution of returns and variance as a function of time, conditional on the initial value of variance. The solution is obtained in two different ways: using the method of characteristics [13] and the method of path integrals [14, 15, 16]. The latter is more familiar to physicists working in finance [12, 17].

While returns are readily known from a financial time series data, variance is not given directly, so it acts as a hidden stochastic variable. Thus, we integrate the joint probability distribution over variance and obtain the marginal probability distribution of returns unconditional on variance. The latter distribution can

be directly compared with financial data. We find an excellent agreement between our results and the Dow-Jones data for the period of 1982–2001. Using only four fitting parameters, our equations very well reproduce the probability distribution of returns for time lags between 1 and 250 trading days. This is in contrast to popular ARCH, GARCH, EGARCH, TARCH, and similar models, where the number of parameters can easily go to a few tens [18].

Our result for the probability distribution of returns has the form of a one-dimensional Fourier integral, which is easily calculated numerically or, in certain asymptotical limits, analytically. For large returns, we find that the probability distribution is exponential in log-returns, which implies a power-law distribution for returns, and we calculate the time dependence of the corresponding exponents. In the limit of long times, the probability distribution exhibits scaling. It becomes a function of a single combination of return and time, with the scaling function expressed in terms of a Bessel function. The Dow-Jones data follow the predicted scaling function for seven orders of magnitude.

The original theory of option pricing was developed by Black and Scholes for the geometric Brownian motion model. Numerous attempts to improve it using stochastic volatility models have been made [8, 9, 10, 11, 12]. Particularly, option pricing for the same model as in our paper was investigated by Heston [11]. Empirical studies [19] show that Heston’s theory fares better than the Black-Scholes model, but still does not fully capture the real-market option prices. Since our paper gives a closed-form time-dependent expression for the probability distribution of returns that agrees with financial data, it can serve as a starting point for a better theory of option pricing.

II. THE MODEL

We consider a stock, whose price S_t , as a function of time t , obeys the stochastic differential equation of a geometric (multiplicative) Brownian motion [1]:

$$dS_t = \mu S_t dt + \sigma_t S_t dW_t^{(1)}. \quad (1)$$

*Electronic address: adragul@physics.umd.edu

†Electronic address: yakovenk@physics.umd.edu

Here the subscript t indicates time dependence, μ is the drift parameter, $W_t^{(1)}$ is the standard random Wiener process¹, and σ_t is a time-dependent parameter, called the stock volatility, which characterizes the noisiness of the Wiener process.

Since any solution of (1) depends only on σ_t^2 , it is convenient to introduce the new variable $v_t = \sigma_t^2$, which is called the variance. We assume that v_t obeys the following mean-reverting stochastic differential equation:

$$dv_t = -\gamma(v_t - \theta) dt + \kappa\sqrt{v_t} dW_t^{(2)}. \quad (2)$$

Here θ is the long-time mean of v , γ is the rate of relaxation to this mean, $W_t^{(2)}$ is the standard Wiener process, and κ is a parameter that we call the variance noise. Eq. (2) is known in financial literature as the Cox-Ingersoll-Ross (CIR) process and in mathematical statistics as the Feller process [8, p. 42]. Alternative equations for v_t , with the last term in (2) replaced by $\kappa dW_t^{(2)}$ or $\kappa v_t dW_t^{(2)}$, are also discussed in literature [9]. However, in this paper, we study only the case given by Eq. (2).

We take the Wiener process appearing in (2) to be correlated with the Wiener process in (1):

$$dW_t^{(2)} = \rho dW_t^{(1)} + \sqrt{1 - \rho^2} dZ_t, \quad (3)$$

where Z_t is a Wiener process independent of $W_t^{(1)}$, and $\rho \in [-1, 1]$ is the correlation coefficient. A negative correlation ($\rho < 0$) between $W_t^{(1)}$ and $W_t^{(2)}$ is known as the leverage effect [8, p. 41].

It is convenient to change the variable in (1) from price S_t to log-return $r_t = \ln(S_t/S_0)$. Using Itô's formula [20], we obtain the equation satisfied by r_t :

$$dr_t = \left(\mu - \frac{v_t}{2} \right) dt + \sqrt{v_t} dW_t^{(1)}. \quad (4)$$

The parameter μ can be eliminated from (4) by changing the variable to $x_t = r_t - \mu t$, which measures log-returns relative to the growth rate μ :

$$dx_t = -\frac{v_t}{2} dt + \sqrt{v_t} dW_t^{(1)}. \quad (5)$$

Where it does not cause confusion with r_t , we use the term “log-return” also for the variable x_t .

Equations (5) and (2) define a two-dimensional stochastic process for the variables x_t and v_t . This process is characterized by the transition probability $P_t(x, v | v_i)$ to have log-return x and variance v at time t given the initial log-return $x = 0$ and variance v_i at $t = 0$. Time evolution of $P_t(x, v | v_i)$ is governed by the

Fokker-Planck (or forward Kolmogorov) equation [20]

$$\begin{aligned} \frac{\partial}{\partial t} P &= \gamma \frac{\partial}{\partial v} [(v - \theta)P] + \frac{1}{2} \frac{\partial}{\partial x} (vP) \\ &+ \rho \kappa \frac{\partial^2}{\partial x \partial v} (vP) + \frac{1}{2} \frac{\partial^2}{\partial x^2} (vP) + \frac{\kappa^2}{2} \frac{\partial^2}{\partial v^2} (vP). \end{aligned} \quad (6)$$

The initial condition for (6) is a product of two delta functions

$$P_{t=0}(x, v | v_i) = \delta(x) \delta(v - v_i). \quad (7)$$

The variance v is a positive quantity, so Eq. (6) is defined only for $v > 0$. However, when solving (6), it is convenient to extend the domain of v so that $v \in (-\infty, \infty)$. If $2\gamma\theta > \kappa^2$, such an extension does not change the solution of the equation, because, given that $P = 0$ for $v < 0$ at the initial time $t = 0$, the condition $P_t(x, v < 0) = 0$ is preserved for all later times $t > 0$. In order to demonstrate this, let us consider (6) in the limit $v \rightarrow 0$:

$$\frac{\partial}{\partial t} P = - \left(\gamma\theta - \frac{\kappa^2}{2} \right) \frac{\partial P}{\partial v} + \gamma P + \rho \kappa \frac{\partial P}{\partial x}. \quad (8)$$

Eq. (8) is a first-order partial differential equation (PDE), which describes propagation of P from negative v to positive v with the positive velocity $\gamma\theta - \kappa^2/2$. Thus, the nonzero function $P(x, v > 0)$ does not propagate to $v < 0$, and $P_t(x, v < 0)$ remains zero at all times t . Alternatively, it is possible to show [1, p. 67] that, if $2\gamma\theta > \kappa^2$, the random process (2) starting in the domain $v > 0$ can never reach the domain $v < 0$.

The probability distribution of the variance itself, $\Pi_t(v) = \int dx P_t(x, v)$, satisfies the equation

$$\frac{\partial}{\partial t} \Pi_t(v) = \frac{\partial}{\partial v} [\gamma(v - \theta)\Pi_t(v)] + \frac{\kappa^2}{2} \frac{\partial^2}{\partial v^2} [v\Pi_t(v)], \quad (9)$$

which is obtained from (6) by integration over x . Eq. (9) has the stationary solution

$$\Pi_*(v) = \frac{\alpha^{\beta+1}}{\Gamma(\alpha)} v^\beta e^{-\alpha v}, \quad \alpha = \frac{2\gamma}{\kappa^2}, \quad \beta = \alpha\theta - 1, \quad (10)$$

which is the Gamma distribution. The maximum of $\Pi_*(v)$ is reached at $v_{\max} = \beta/\alpha = \theta - \kappa^2/2\gamma$. The width w of $\Pi_*(v)$ can be estimated using the curvature at the maximum $w \approx (\kappa^2/2\gamma)\sqrt{2\gamma\theta/\kappa^2 - 1}$. The shape of $\Pi_*(v)$ is characterized by the dimensionless ratio

$$\chi = \frac{v_{\max}}{w} = \sqrt{\frac{2\gamma\theta}{\kappa^2} - 1}. \quad (11)$$

When $2\gamma\theta/\kappa^2 \rightarrow \infty$, $\chi \rightarrow \infty$ and $\Pi_*(v) \rightarrow \delta(v - \theta)$.

III. SOLUTION OF THE FOKKER-PLANCK EQUATION

Since x appears in (6) only in the derivative operator $\partial/\partial x$, it is convenient to make the Fourier transform

$$P_t(x, v | v_i) = \frac{1}{2\pi} \int_{-\infty}^{+\infty} dp_x e^{ip_x x} \overline{P}_{t, p_x}(v | v_i). \quad (12)$$

¹ The infinitesimal increments of the Wiener process dW_t are normally distributed (Gaussian) random variables with zero mean and the variance equal to dt .

Inserting (12) into (6), we find

$$\begin{aligned} \frac{\partial}{\partial t} \bar{P} &= \gamma \frac{\partial}{\partial v} [(v - \theta) \bar{P}] \\ &- \left[\frac{p_x^2 - ip_x}{2} v - i\rho\kappa p_x \frac{\partial}{\partial v} v - \frac{\kappa^2}{2} \frac{\partial^2}{\partial v^2} v \right] \bar{P}. \end{aligned} \quad (13)$$

Eq. (13) is simpler than (6), because the number of variables has been reduced to two, v and t , whereas p_x only plays the role of a parameter.

Since Eq. (13) is linear in v and quadratic in $\partial/\partial v$, it can be simplified by taking the Fourier transform over v

$$\bar{P}_{t,p_x}(v | v_i) = \frac{1}{2\pi} \int_{-\infty}^{+\infty} dp_v e^{ip_v v} \tilde{P}_{t,p_x}(p_v | v_i). \quad (14)$$

The PDE satisfied by $\tilde{P}_{t,p_x}(p_v | v_i)$ is of the first order

$$\left[\frac{\partial}{\partial t} + \left(\Gamma p_v + \frac{i\kappa^2}{2} p_v^2 + \frac{ip_x^2 - p_x}{2} \right) \frac{\partial}{\partial p_v} \right] \tilde{P} = -i\gamma\theta p_v \tilde{P}, \quad (15)$$

where we introduced the notation

$$\Gamma = \gamma + i\rho\kappa p_x. \quad (16)$$

Eq. (15) has to be solved with the initial condition

$$\tilde{P}_{t=0,p_x}(p_v | v_i) = \exp(-ip_v v_i). \quad (17)$$

The solution of the PDE (15) is given by the method of characteristics [13]:

$$\tilde{P}_{t,p_x}(p_v | v_i) = \exp \left(-ip_v(0)v_i - i\gamma\theta \int_0^t d\tau \tilde{p}_v(\tau) \right), \quad (18)$$

where the function $\tilde{p}_v(\tau)$ is the solution of the characteristic (ordinary) differential equation

$$\frac{d\tilde{p}_v(\tau)}{d\tau} = \Gamma \tilde{p}_v(\tau) + \frac{i\kappa^2}{2} \tilde{p}_v^2(\tau) + \frac{i}{2} (p_x^2 - ip_x) \quad (19)$$

with the boundary condition $\tilde{p}_v(t) = p_v$ specified at $\tau = t$. The solution (18) can be also obtained using the method of path integrals described in Appendix A. The differential equation (19) is of the Riccati type with constant coefficients [21], and its solution is

$$\tilde{p}_v(\tau) = -i \frac{2\Omega}{k^2} \frac{1}{\zeta e^{\Omega(t-\tau)} - 1} + i \frac{\Gamma - \Omega}{k^2}, \quad (20)$$

where we introduced the frequency

$$\Omega = \sqrt{\Gamma^2 + \kappa^2(p_x^2 - ip_x)}. \quad (21)$$

and the coefficient

$$\zeta = 1 - i \frac{2\Omega}{\kappa^2 p_v - i(\Gamma - \Omega)}. \quad (22)$$

Substituting (20) into (18) and taking the Fourier transforms (12) and (14), we get the solution

$$\begin{aligned} P_t(x, v | v_i) &= \frac{1}{(2\pi)^2} \iint_{-\infty}^{+\infty} dp_x dp_v e^{ip_x x + ip_v v} \\ &\times \exp \left\{ -\tilde{p}_v(0)v_i + \frac{\gamma\theta(\Gamma - \Omega)t}{\kappa^2} - \frac{2\gamma\theta}{\kappa^2} \ln \frac{\zeta - e^{-\Omega t}}{\zeta - 1} \right\} \end{aligned} \quad (23)$$

of the original Fokker-Planck equation (6) with the initial condition (7), where $\tilde{p}_v(\tau = 0)$ is given by (20).

IV. AVERAGING OVER VARIANCE

Normally we are interested only in log-returns x and do not care about variance v . Moreover, whereas log-returns are directly known from financial data, variance is a hidden stochastic variable that has to be estimated. Inevitably, such an estimation is done with some degree of uncertainty, which precludes a clear-cut direct comparison between $P(x, v, t | v_i)$ and financial data. Thus we introduce the probability distribution

$$P_t(x | v_i) = \int_{-\infty}^{+\infty} dv P_t(x, v | v_i), \quad (24)$$

where the hidden variable v is integrated out. The integration of (23) over v generates the delta-function $\delta(p_v)$, which effectively sets $p_v = 0$. Substituting the coefficient ζ from (22) with $p_v = 0$ into (23), we find

$$\begin{aligned} P_t(x | v_i) &= \frac{1}{2\pi} \int_{-\infty}^{+\infty} dp_x e^{ip_x x - v_i \frac{p_x^2 - ip_x}{1 + \Omega \coth(\Omega t/2)}} \\ &\times e^{-\frac{2\gamma\theta}{\kappa^2} \ln(\cosh \frac{\Omega t}{2} + \frac{\gamma}{\Omega} \sinh \frac{\Omega t}{2}) + \frac{2\Gamma\theta t}{\kappa^2}}. \end{aligned} \quad (25)$$

To check the validity of (25), let us consider the case $\kappa = 0$. In this case, the stochastic term in (2) is absent, so the time evolution of variance is deterministic:

$$v(t) = \theta + (v_i - \theta)e^{-\gamma t}. \quad (26)$$

Then process (5) gives a Gaussian distribution for x ,

$$P_t^{(\kappa=0)}(x | v_i) = \frac{1}{\sqrt{2\pi t \bar{v}_t}} \exp \left(-\frac{(x + \bar{v}_t t/2)^2}{2\bar{v}_t t} \right), \quad (27)$$

with the time-averaged variance $\bar{v}_t = \frac{1}{t} \int_0^t d\tau v(\tau)$. Eq. (27) demonstrates that the probability distribution of stock price S is log-normal in the case $\kappa = 0$. On the other hand, by taking the limit $\kappa \rightarrow 0$ and integrating over p_x in (25), we reproduce the same expression (27).

Eq. (25) cannot be directly compared with financial time series data, because it depends on the unknown initial variance v_i . In order to resolve this problem, we assume that v_i has the stationary probability distribution $\Pi_*(v_i)$, which is given by (10).² Thus we introduce

² An attempt to determine the probability distribution of volatility empirically for the S&P 500 stock index was done in Ref. [22].

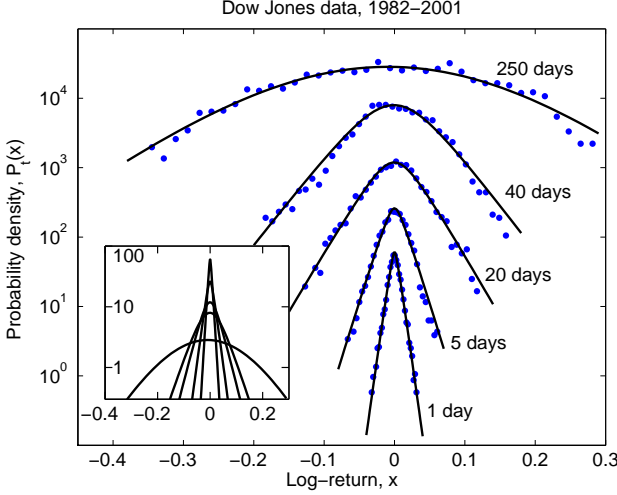


FIG. 1: Probability distribution $P_t(x)$ of log-return x for different time lags t . Points: The Dow-Jones data for $t = 1, 5, 20, 40$, and 250 trading days. Solid lines: Fit of the data with Eqs. (29) and (30). For clarity, the data points and the curves for successive t are shifted up by the factor of 10 each. The inset shows the curves without vertical shift.

the probability distribution $P_t(x)$ by averaging (25) over v_i with the weight $\Pi_*(v_i)$:

$$P_t(x) = \int_0^\infty dv_i \Pi_*(v_i) P_t(x | v_i). \quad (28)$$

The integral over v_i is similar to the one of the Gamma function and can be taken explicitly. The final result is the Fourier integral

$$P_t(x) = \frac{1}{2\pi} \int_{-\infty}^{+\infty} dp_x e^{ip_x x + F_t(p_x)} \quad (29)$$

with

$$F_t(p_x) = \frac{\gamma\Gamma\theta t}{\kappa^2} - \frac{2\gamma\theta}{\kappa^2} \ln \left[\frac{\cosh \frac{\Omega t}{2} + \frac{\gamma}{\Omega} \sinh \frac{\Omega t}{2}}{\cosh \frac{\Omega t}{2} + \frac{\Gamma}{\Omega} \sinh \frac{\Omega t}{2}} \right] - \frac{2\gamma\theta}{\kappa^2} \ln \left[\cosh \frac{\Omega t}{2} + \frac{\Omega^2 - \Gamma^2 + 2\gamma\Gamma}{2\gamma\Omega} \sinh \frac{\Omega t}{2} \right]. \quad (30)$$

The variable p_x enters (30) via the variables Γ from (16) and Ω from (21). It is easy to check that $P_t(x)$ is real, because $\text{Re}F$ is an even function of p_x and $\text{Im}F$ is an odd one. One can also check that $F_t(p_x = 0) = 0$, which implies that $P_t(x)$ is correctly normalized at all times: $\int dx P_t(x) = 1$. The second term in the r.h.s. of (30) vanishes when $\rho = 0$, i.e. when there are no correlations between stock price and variance. The simplified result for the case $\rho = 0$ is given in Appendix B by Eqs. (B1), (B2), and (B3).

Eqs. (29) and (30) for the probability distribution $P_t(x)$ of log-return x at time t are the central analytical result of the paper. The integral in (29) can be calculated numerically or, in certain regimes discussed in Secs.

V and VI, analytically. In Fig. 1, the calculated function $P_t(x)$, shown by solid lines, is compared with the Dow-Jones data, shown by dots. (Technical details of the data analysis are discussed in Sec. VII.) Fig. 1 demonstrates that, with a fixed set of the parameters $\gamma, \theta, \kappa, \mu$, and ρ , Eqs. (29) and (30) very well reproduce the distribution of log-returns x of the Dow-Jones index for all times t . In the log-linear scale of Fig. 1, the tails of $\ln P_t(x)$ vs. x are straight lines, which means that the tails of $P_t(x)$ are exponential in x . For short times, the distribution is narrow, and the slopes of the tails are nearly vertical. As time progresses, the distribution broadens and flattens.

V. ASYMPTOTIC BEHAVIOR FOR LONG TIME t

Eq. (2) implies that variance reverts to the equilibrium value θ within the characteristic relaxation time $1/\gamma$. In this section, we consider the asymptotic limit where time t is much longer than the relaxation time: $\gamma t \gg 2$. According to (16) and (21), this condition also implies that $\Omega t \gg 2$. Then Eq. (30) reduces to

$$F_t(p_x) \approx \frac{\gamma\theta t}{\kappa^2} (\Gamma - \Omega). \quad (31)$$

Let us change of the variable of integration in (29) to

$$p_x = \frac{\omega_0}{\kappa\sqrt{1-\rho^2}} \tilde{p}_x + ip_0, \quad (32)$$

where

$$p_0 = \frac{\kappa - 2\rho\gamma}{2\kappa(1-\rho^2)}, \quad \omega_0 = \sqrt{\gamma^2 + \kappa^2(1-\rho^2)p_0^2}. \quad (33)$$

Substituting (32) into (16), (21), and (31), we transform (29) to the following form

$$P_t(x) = \frac{\omega_0 e^{-p_0 x + \Lambda t}}{\pi\kappa\sqrt{1-\rho^2}} \int_0^\infty d\tilde{p}_x \cos(A\tilde{p}_x) e^{-B\sqrt{1+\tilde{p}_x^2}}, \quad (34)$$

where

$$A = \frac{\omega_0}{\kappa\sqrt{1-\rho^2}} \left(x + \rho \frac{\gamma\theta t}{\kappa} \right), \quad B = \frac{\gamma\theta\omega_0 t}{\kappa^2}, \quad (35)$$

and

$$\Lambda = \frac{\gamma\theta}{2\kappa^2} \frac{2\gamma - \rho\kappa}{1 - \rho^2}. \quad (36)$$

According to [23], the integral in (34) is equal to $BK_1(\sqrt{A^2 + B^2})/\sqrt{A^2 + B^2}$, where K_1 is the first-order modified Bessel function.

Thus, Eq. (29) in the limit $\gamma t \gg 2$ can be represented in the scaling form

$$P_t(x) = N_t e^{-p_0 x} P_*(z), \quad P_*(z) = K_1(z)/z, \quad (37)$$

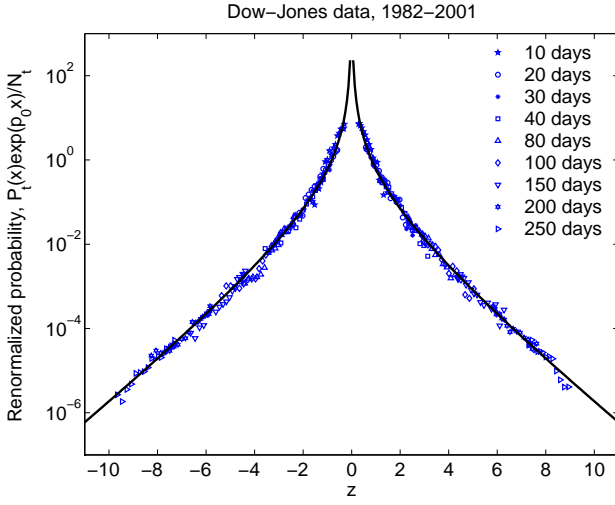


FIG. 2: Renormalized probability density $P_t(x)e^{p_0x}/N_t$ plotted as a function of the scaling argument z given by (38). Solid line: The scaling function $P_*(z) = K_1(z)/z$ from (37), where K_1 is the first-order modified Bessel function. Symbols: The Dow-Jones data for different time lags t .

where the argument $z = \sqrt{A^2 + B^2}$ is

$$z = \frac{\omega_0}{\kappa} \sqrt{\frac{(x + \rho\gamma\theta t/\kappa)^2}{1 - \rho^2} + \left(\frac{\gamma\theta t}{\kappa}\right)^2}, \quad (38)$$

and the time-dependent normalization factor N_t is

$$N_t = \frac{\omega_0^2 \gamma \theta t}{\pi \kappa^3 \sqrt{1 - \rho^2}} e^{\Lambda t}, \quad (39)$$

Eq. (37) demonstrates that, up to the factors N_t and e^{-p_0x} , the dependence of $P_t(x)$ on the two arguments x and t is given by the function $P_*(z)$ of the single scaling argument z in (38). Thus, when plotted as a function of z , the data for different x and t should collapse on the single universal curve $P_*(z)$. This is beautifully illustrated by Fig. 2, where the Dow-Jones data for different time lags t follows the curve $P_*(z)$ for seven decades.

In the limit $z \gg 1$, we can use the asymptotic expression [23] $K_1(z) \approx e^{-z} \sqrt{\pi/2z}$ in (37) and take the logarithm of P . Keeping only the leading term proportional to z and omitting the subleading term proportional to $\ln z$, we find

$$\ln \frac{P_t(x)}{N_t} \approx -p_0x - z \quad \text{for } z \gg 1. \quad (40)$$

Let us examine Eq. (40) for large and small $|x|$.

In the first case $|x| \gg \gamma\theta t/\kappa$, Eq. (38) gives $z \approx \omega_0|x|/\kappa\sqrt{1 - \rho^2}$, so Eq. (40) becomes

$$\ln \frac{P_t(x)}{N_t} \approx -p_0x - \frac{\omega_0}{\kappa\sqrt{1 - \rho^2}}|x|. \quad (41)$$

Thus, the probability distribution $P_t(x)$ has the exponential tails (41) for large log-returns $|x|$. Notice that, in the

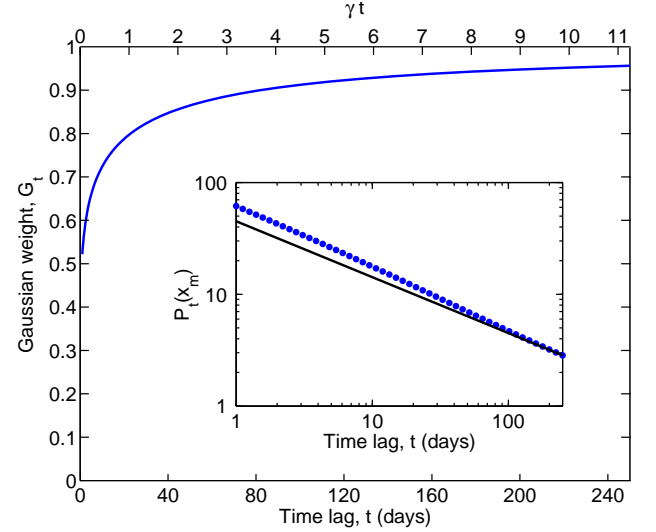


FIG. 3: The fraction G_t of the total probability contained in the Gaussian part of $P_t(x)$ vs. time lag t . Inset: Time dependence of the probability density at maximum $P_t(x_m)$ (points), compared with the Gaussian $t^{-1/2}$ behavior (solid line).

considered limit $\gamma t \gg 2$, the slopes $d \ln P/dx$ of the exponential tails (41) do not depend on time t . Because of p_0 , the slopes (41) for positive and negative x are not equal, thus the distribution $P_t(x)$ is not symmetric with respect to up and down price changes. According to (33), this asymmetry is enhanced by a negative correlation $\rho < 0$ between stock price and variance.

In the second case $|x| \ll \gamma\theta t/\kappa$, by Taylor-expanding z in (38) near its minimum and substituting the result into (40), we get

$$\ln \frac{P_t(x)}{N'_t} \approx -p_0x - \frac{\omega_0(x + \rho\gamma\theta t/\kappa)^2}{2(1 - \rho^2)\gamma\theta t}, \quad (42)$$

where $N'_t = N_t \exp(-\omega_0\gamma\theta t/\kappa^2)$. Thus, for small log-returns $|x|$, the probability distribution $P_t(x)$ is Gaussian with the width increasing linearly in time. The maximum of $P_t(x)$ in (42) is achieved at

$$x_m(t) = -\frac{\gamma\theta t}{2\omega_0} \left(1 + 2 \frac{\rho(\omega_0 - \gamma)}{\kappa}\right). \quad (43)$$

Eq. (43) gives the most probable log-return $x_m(t)$ at time t , and the coefficient in front of t constitutes a correction to the average growth rate μ , so that the actual growth rate is $\bar{\mu} = \mu + dx_m/dt$.

As Fig. 1 illustrates, $\ln P_t(x)$ is indeed linear in x for large $|x|$ and quadratic for small $|x|$, in agreement with (41) and (42). As time progresses, the distribution, which has the scaling form (37) and (38), broadens. Thus, the fraction G_t of the total probability contained in the parabolic (Gaussian) portion of the curve increases, as illustrated in Fig. 3. (The procedure of calculating G_t is explained in Appendix B.) Fig. 3 shows that, at sufficiently long times, the total probability contained in the

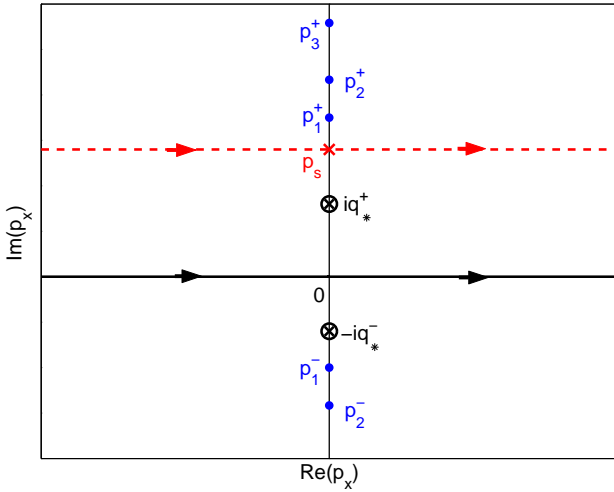


FIG. 4: Complex plane of p_x . Dots: The singularities of $F_t(p_x)$. Circled crosses: The accumulation points $\pm iq_*^\pm$ of the singularities in the limit $\gamma t \gg 2$. Cross: Saddle point p_s , which is located in the upper half-plane for $x > 0$. Dashed line: The contour of integration displaced from the real axis in order to pass through the saddle point p_s .

non-Gaussian tails becomes negligible, which is known in literature [6]. The inset in Fig. 3 illustrates that the time dependence of the probability density at maximum, $P_t(x_m)$, is close to $t^{-1/2}$, which is characteristic for a Gaussian evolution.

VI. ASYMPTOTIC BEHAVIOR FOR LARGE LOG-RETURN x

In the complex plane of p_x , function $F(p_x)$ becomes singular at the points p_x where the argument of any logarithm in (30) vanishes. These points are located on the imaginary axis of p_x and are shown by dots in Fig. 4. The singularity closest to the real axis is located on the positive (negative) imaginary axis at the point p_1^+ (p_1^-). At these two points, the argument of the last logarithm in (30) vanishes, and we can approximate $F(p_x)$ by the dominant, singular term: $F(p_x) \approx -(2\gamma\theta/\kappa^2) \ln(p_x - p_1^\pm)$.

For large $|x|$, the integrand of (29) oscillates very fast as a function of p_x . Thus, we can evaluate the integral using the method of stationary phase [21] by shifting the contour of integration so that it passes through a saddle point of the argument $ip_x x + F(p_x)$ of the exponent in (29). The saddle point position p_s , shown in Fig. 4 by the cross, is determined by the equation

$$ix = - \frac{dF(p_x)}{dp_x} \Big|_{p_x=p_s} \approx \frac{2\gamma\theta}{\kappa^2} \times \begin{cases} \frac{1}{p_s - p_1^+}, & x > 0, \\ \frac{1}{p_s - p_1^-}, & x < 0. \end{cases} \quad (44)$$

For a large $|x|$ such that $|xp_1^\pm| \gg 2\gamma\theta/\kappa^2$, the saddle point p_s is very close to the singularity point: $p_s \approx p_1^\pm$

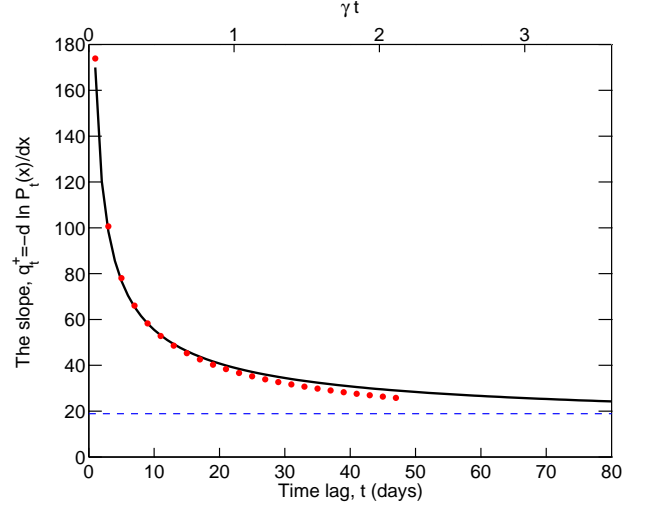


FIG. 5: Solid line: The slope $q_t^+ = -d \ln P_t(x)/dx$ of the exponential tail for $x > 0$ as a function of time. Points: The asymptotic approximation (47) for the slope in the limit $\gamma t \ll 2$. Dashed line: The saturation value q_*^+ for $\gamma t \gg 2$, Eq. (46).

for $x > 0$ and $p_s \approx p_1^-$ for $x < 0$. Then the asymptotic expression for the probability distribution is

$$P_t(x) \sim \begin{cases} e^{-xq_t^+}, & x > 0, \\ e^{xq_t^-}, & x < 0, \end{cases} \quad (45)$$

where $q_t^\pm = \mp ip_1^\pm(t)$ are real and positive. Eq. (45) shows that, for all times t , the tails of the probability distribution $P_t(x)$ for large $|x|$ are exponential. The slopes of the exponential tails, $q^\pm = \mp d \ln P_t(x)/dx$, are determined by the positions $p_1^\pm(t)$ of the singularities closest to the real axis.

These positions $p_1^\pm(t)$ and, thus, the slopes q_t^\pm depend on time t . For times much shorter than the relaxation time ($\gamma t \ll 2$), the singularities lie far away from the real axis. As time increases, the singularities move along the imaginary axis toward the real axis. Finally, for times much longer than the relaxation time ($\gamma t \gg 2$), the singularities approach limiting points: $p_1^\pm \rightarrow \pm iq_*^\pm$, which are shown in Fig. 4 by circled crosses. Thus, as illustrated in Fig. 5, the slopes q_t^\pm monotonously decrease in time and saturate at long times:

$$q_t^\pm \rightarrow q_*^\pm = \pm p_0 + \frac{\omega_0}{\kappa\sqrt{1-\rho^2}} \quad \text{for } \gamma t \gg 2. \quad (46)$$

The slopes (46) are in agreement with Eq. (41) valid for $\gamma t \gg 2$. The time dependence q_t^\pm at short times can be also found analytically:

$$q_t^\pm \approx \pm p_0 + \sqrt{p_0 + \frac{4\gamma}{\kappa^2(1-\rho^2)t}} \quad \text{for } \gamma t \ll 2. \quad (47)$$

The dotted curve in Fig. 5 shows that Eq. (47) works very well for short times t , where the slope diverges at $t \rightarrow 0$.

VII. COMPARISON WITH THE DOW-JONES TIME SERIES

To test the model against financial data, we downloaded daily closing values of the Dow-Jones industrial index for the period of 20 years from 1 January 1982 to 31 December 2001 from the Web site of Yahoo [24]. The data set contains 5049 points, which form the time series $\{S_\tau\}$, where the integer time variable τ is the trading day number. We do not filter the data for short days, such as those before holidays.

Given $\{S_\tau\}$, we use the following procedure to extract the probability density $P_t^{(DJ)}(r)$ of log-return r for a given time lag t . For the fixed t , we calculate the set of log-returns $\{r_\tau = \ln S_{\tau+t}/S_\tau\}$ for all possible times τ . Then we partition the r -axis into equally spaced bins of the width Δr and count the number of log-returns r_τ belonging to each bin. In this process, we omit the bins with occupation numbers less than five, because we consider such a small statistics unreliable. Only less than 1% of the entire data set is omitted in this procedure. Dividing the occupation number of each bin by Δr and by the total occupation number of all bins, we obtain the probability density $P_t^{(DJ)}(r)$ for a given time lag t . To find $P_t^{(DJ)}(x)$, we replace $r \rightarrow x + \mu t$.

Assuming that the system is ergodic, so that ensemble averaging is equivalent to time averaging, we compare $P_t^{(DJ)}(x)$ extracted from the time series data and $P_t(x)$ calculated in previous sections, which describes ensemble distribution. In the language of mathematical statistics, we compare our theoretically derived population distribution with the sample distribution extracted from the time series data. We determine parameters of the model by minimizing the mean-square deviation $\sum_{x,t} |\ln P_t^{(DJ)}(x) - \ln P_t(x)|^2$, where the sum is taken over all available x and $t = 1, 5, 20, 40$, and 250 days. These values of t are selected because they represent different regimes: $\gamma t \ll 1$ for $t = 1$ and 5 days, $\gamma t \approx 1$ for $t = 20$ days, and $\gamma t \gg 1$ for $t = 40$ and 250 days. As Figs. 1 and 2 illustrate, our expression (29) and (30) for the probability density $P_t(x)$ agrees with the data very well, not only for the selected five values of time t , but for the whole time interval from 1 to 250 trading days. However, we cannot extend this comparison to t longer than 250 days, which is approximately 1/20 of the entire range of the data set, because we cannot reliably extract $P_t^{(DJ)}(x)$ from the data when t is too long.

The values obtained for the four fitting parameters $(\gamma, \theta, \kappa, \mu)$ are given in Table I. Within the scattering of the data, we do not find any discernible difference between the fits with the correlation coefficient ρ being zero or slightly different from zero. Thus, we conclude that the correlation ρ between the noise terms for stock price and variance in Eq. (3) is practically zero, if it exists at all. Our conclusion is in contrast with the value $\rho = 0.58$ found in [25] by fitting the leverage correlation function introduced in [26]. Further study is necessary in order

TABLE I: Parameters of the model obtained from the fit of the Dow-Jones data. We also find $\rho = 0$ for the correlation coefficient and $1/\gamma = 22.2$ trading days for the relaxation time of variance.

Units	γ	θ	κ	μ
1/day	4.50×10^{-2}	8.62×10^{-5}	2.45×10^{-3}	5.67×10^{-4}
1/year	11.35	0.022	0.618	0.143

to resolve this discrepancy. Nevertheless, all theoretical curves shown in our paper are calculated for $\rho = 0$, and they fit the data very well.

All four parameters $(\gamma, \theta, \kappa, \mu)$ shown in Table I have the dimensionality of 1/time. The first line of the Table gives their values in the units of 1/day, as originally determined in our fit. The second line shows the annualized values of the parameters in the units of 1/year, where we utilize the average number of 252.5 trading days per calendar year to make the conversion. The relaxation time of variance is equal to $1/\gamma = 22.2$ trading days = 4.4 weeks \approx 1 month, where we took into account that 1 week = 5 trading days. Thus, we find that variance has a rather long relaxation time, of the order of one month, which is in agreement with the conclusion of Ref. [25].

Using the numbers given in Table I, we find the value of the parameter $2\gamma\theta/\kappa^2 = 1.296$. Since this parameter is greater than one, the stochastic process (2) never reaches the domain $v < 0$, as discussed in Sec. II.

The effective growth rate of stock prices is determined by the coordinate $r_m(t)$ where the probability density $P_t(r_m)$ is maximal. Using the relation $r_m = x_m + \mu t$ and Eq. (43), we find that the actual growth rate is $\bar{\mu} = \mu - \gamma\theta/2\omega_0 = 13\%$ per year. This number coincides with the average growth rate of the Dow-Jones index obtained by a simple fit of the time series $\{S_\tau\}$ with an exponential function of τ . The effective stock growth rate $\bar{\mu}$ is comparable with the average stock volatility after one year $\sigma = \sqrt{\theta} = 14.7\%$. Moreover, the parameter (11), which characterizes the width of the stationary distribution of variance, is equal to $\chi = 0.54$. This means that the distribution of variance is broad, and variance can easily fluctuate to a value twice greater than the average value θ . Thus, even though the average growth rate of stock index is positive, there is a substantial probability $\int_{-\infty}^0 dr P_t(r) = 17.7\%$ to have negative growth for $t = 1$ year.

According to (46), the asymmetry between the slopes of exponential tails for positive and negative x is given by the parameter p_0 , which is equal to 1/2 when $\rho = 0$ (see also the discussion of Eq. (B1) in Appendix B). The origin of this asymmetry can be traced back to the transformation from (1) to (4) using Itô's formula. It produces the term $0.5v_t dt$ in the r.h.s. of (4), which then generates the second term in the r.h.s. of (6). The latter term is the only source of asymmetry in x of $P_t(x)$ when $\rho = 0$. However, in practice, the asymmetry of the slopes $p_0 = 1/2$ is quite small (about 2.7%) compared with the

average slope $q_*^\pm \approx \omega_0/\kappa = 18.4$.

VIII. CONCLUSIONS

We derived an analytical solution for the probability distribution $P_t(x)$ of log-returns x as a function of time t for the model of a geometrical Brownian motion with stochastic variance. The final result has the form of a one-dimensional Fourier integral (29) and (30). [In the case $\rho = 0$, the equations have the simpler form (B1), (B2), and (B3).] Numerical evaluation of the integral (29) is simple compared with computationally-intensive numerical solution of the original Fokker-Planck PDE or Monte-Carlo simulation of the stochastic processes.

Our result agrees very well with the Dow-Jones data, as shown in Fig. 1. Comparing the theory and the data, we determine the four (non-zero) fitting parameters of the model, particularly the variance relaxation time $1/\gamma = 22.2$ days. For time longer than $1/\gamma$, our theory predicts scaling behavior (37) and (38), which the Dow-Jones data indeed exhibits over seven orders of magnitude, as shown in Fig. 2. The scaling function $P_*(z) = K_1(z)/z$ is expressed in terms of the first-order modified Bessel function K_1 . Previous estimates in literature of the relaxation time of volatility using various indirect indicators range from 1.5 days [8, p. 80] to less than one day and more than few tens of days [2, p. 70] for S&P 500 and 73 days for the half-life of the Dow-Jones index [7]. Since we have a very good fit of the entire probability distribution function for times from 1 to 250 trading days, we believe that our estimate, 22.2 days, is much more reliable. A close value of 19.6 days was found in Ref. [25].

As Fig. 1 shows, the probability distribution $P_t(x)$ is exponential in x for large $|x|$, where it is characterized by time-dependent slopes $d \ln P/dx$. The theoretical analysis presented in Sec. VI shows that the slopes are determined by the singularities of the function $F_t(p_x)$ from (30) in the complex plane of p_x that are closest to the real axis. The calculated time dependence of the slopes $d \ln P/dx$, shown in Fig. 5, agrees with the data very well, which further supports our statement that $1/\gamma = 22.2$ days. Exponential tails in the probability distribution of stock log-returns have been noticed in literature before [2, p. 61], [27], however time dependence of the slopes has not been recognized and analyzed theoretically. In Ref. [6], the power-law behavior of the tails has been emphasized. However, the data for S&P 500 were analyzed in Ref. [6] only for short time lags t , typically shorter than one day. On the other hand, our data analysis is performed for the time lags longer than one day, so the results cannot be directly compared.

Our analytical expression for the probability distribution of returns can be utilized to calculate option pricing. Notice that it is not necessary to introduce the ad-hoc function $\lambda(S, v, t)$, the market-price of risk, as is typically done in literature [1, 8, 9, 10, 11], because now $P_t(x)$ is

known explicitly. Using the true probability distribution of returns $P_t(x)$ should improve option pricing compared with the previous efforts in literature.

Although we tested our model for the Dow-Jones index, there is nothing specific in the model which indicates that it applies only to stock market data. It would be interesting to see how the model performs when applied to other time series, for example, the foreign exchange data [28], which also seem to exhibit exponential tails.

APPENDIX A: PATH-INTEGRAL SOLUTION

The Fokker-Planck equation (13) can be thought of as a Schrödinger equation in imaginary (Euclidean) time:

$$\frac{\partial}{\partial t} \overline{P}_{t,p_x}(v | v_i) = -\hat{H}_{p_x}(\hat{p}_v, \hat{v}) \overline{P}_{t,p_x}(v | v_i) \quad (A1)$$

with the Hamiltonian

$$\hat{H} = \frac{\kappa^2}{2} \hat{p}_v^2 \hat{v} - i\gamma \hat{p}_v(\hat{v} - \theta) + \frac{p_x^2 - ip_x}{2} \hat{v} + \rho \kappa p_x \hat{p}_v \hat{v}. \quad (A2)$$

In (A2) we treat \hat{p}_v and \hat{v} as canonically conjugated operators with the commutation relation $[\hat{v}, \hat{p}_v] = i$. The transition probability $\overline{P}_{p_x}(v, t | v_i)$ is the matrix element of the evolution operator $\exp(-\hat{H}t)$ and has a path-integral representation [14, 15, 16]

$$\overline{P}_{t,p_x}(v | v_i) = \langle v | e^{-\hat{H}t} | v_i \rangle = \int \mathcal{D}v \mathcal{D}p_v e^{S_{p_x}[p_v(\tau), v(\tau)]}. \quad (A3)$$

Here the action functional $S_{p_x}[p_v(\tau), v(\tau)]$ is

$$S_{p_x} = \int_0^t d\tau \{ ip_v(\tau) \dot{v}(\tau) - H_{p_x} [p_v(\tau), v(\tau)] \}, \quad (A4)$$

and the dot denotes the time derivative. The phase-space path integral (A3) is the sum over all possible paths $p_v(\tau)$ and $v(\tau)$ with the boundary conditions $v(\tau = 0) = v_i$ and $v(\tau = t) = v$ imposed on v .

It is convenient to integrate the first term in the r.h.s. of (A4) by parts:

$$S_{p_x} = i[p_v(t)v - \tilde{p}_v(0)v_i] - i\gamma\theta \int_0^t d\tau p_v(\tau) - \int_0^t d\tau \left[i\dot{p}_v(\tau) + \frac{\delta H}{\delta v(\tau)} \right] v(\tau), \quad (A5)$$

where we also separated the terms linear in $v(\tau)$ from the Hamiltonian (A2). Because $v(\tau)$ enters linearly in the action (A5), taking the path integral over $\mathcal{D}v$ generates the delta-functional $\delta[p_v(\tau) - \tilde{p}_v(\tau)]$, where $\tilde{p}_v(\tau)$ is the solution of the ordinary differential equation (19) with a boundary condition specified at $\tau = t$. Taking the path integral over $\mathcal{D}p_v$ resolves the delta-functional, and we find

$$\overline{P}_{t,p_x}(v | v_i) = \int_{-\infty}^{+\infty} \frac{dp_v}{2\pi} e^{i[p_v v - \tilde{p}_v(0)v_i] - i\gamma\theta \int_0^t d\tau \tilde{p}_v(\tau)}, \quad (A6)$$

where $\tilde{p}_v(\tau = t) = p_v$. Eq. (A6) coincides with (18) after the Fourier transform (14).

APPENDIX B: GAUSSIAN WEIGHT

As explained in Sec. VII, the case relevant for comparison with the data is $\rho = 0$. In this case, by shifting the contour of integration in (29) as follows $p_x \rightarrow p_x + i/2$, we find

$$P_t(x) = e^{-x/2} \int_{-\infty}^{+\infty} \frac{dp_x}{2\pi} e^{ip_x x + F_t(p_x)}, \quad (\text{B1})$$

where

$$F_t(p_x) = \frac{\gamma^2 \theta t}{\kappa^2} - \frac{2\gamma\theta}{\kappa^2} \ln \left[\cosh \frac{\Omega t}{2} + \frac{\Omega^2 + \gamma^2}{2\gamma\Omega} \sinh \frac{\Omega t}{2} \right] \quad (\text{B2})$$

and

$$\Omega = \sqrt{\gamma^2 + \kappa^2(p_x^2 + 1/4)}. \quad (\text{B3})$$

Now the function $F_t(p_x)$ is real and symmetric: $F_t(p_x) = F_t(-p_x)$. Thus, the integral in (B1) is a symmetric function of x . So it is clear that the only source of asymmetry of $P_t(x)$ in x is the exponential prefactor in (B1), as discussed at the end of Sec. VII. Eqs. (B1), (B2), and (B3) are much simpler than those for $\rho \neq 0$.

Let us expand the integral in (B1) for small x :

$$P_t(x) \approx e^{-x/2} \left(\mu_0 - \frac{1}{2} \mu_2 x^2 \right), \quad (\text{B4})$$

where the coefficients are the first and the second mo-

ments of $\exp[F_t(p_x)]$

$$\mu_0(t) = \int_{-\infty}^{+\infty} \frac{dp_x}{2\pi} e^{F_t(p_x)}, \quad \mu_2(t) = \int_{-\infty}^{+\infty} \frac{dp_x}{2\pi} p_x^2 e^{F_t(p_x)}. \quad (\text{B5})$$

On the other hand, we know that $P_t(x)$ is Gaussian for small x . So we can write

$$P_t(x) \approx \mu_0 e^{-x/2} e^{-\mu_2 x^2 / 2\mu_0}, \quad (\text{B6})$$

with the same coefficients as in (B4). If we ignore the existence of fat tails and extrapolate (B6) to $x \in (-\infty, \infty)$, the total probability contained in such a Gaussian extrapolation will be

$$G_t = \int_{-\infty}^{+\infty} dx \mu_0 e^{-x/2 - \mu_2 x^2 / 2\mu_0} = \sqrt{\frac{2\pi\mu_0^3}{\mu_2}} e^{\mu_0/8\mu_2}. \quad (\text{B7})$$

Obviously, $G_t < 1$, because the integral (B7) does not take into account the probability contained in the fat tails. Thus, the difference $1 - G_t$ can be taken as a measure of how much the actual distribution $P_t(x)$ deviates from a Gaussian function.

We calculate the moments (B5) numerically for the function F given by (B2), then determine the Gaussian weight G_t from (B7) and plot it in Fig. 3 as a function of time. For $t \rightarrow \infty$, $G_t \rightarrow 1$, i.e. $P_t(x)$ becomes Gaussian for very long time lags, which is known in literature [6]. In the opposite limit $t \rightarrow 0$, $F_t(p_x)$ becomes a very broad function of p_x , so we cannot calculate the moments μ_0 and μ_2 numerically. The singular limit $t \rightarrow 0$ requires an analytical study.

[1] P. Wilmott, *Derivatives* (John Wiley & Sons, New York, 1998).
[2] J. P. Bouchaud and M. Potters, *Theory of Financial Risks* (Cambridge University Press, Cambridge, 2001).
[3] R. N. Mantegna and H. E. Stanley, *An Introduction to Econophysics* (Cambridge University Press, Cambridge, 2000).
[4] J. Voit, *The Statistical Mechanics of Financial Markets* (Springer, Berlin, 2001).
[5] B. B. Mandelbrot, *Journal of Business* **36**, 393 (1963).
[6] R. N. Mantegna and H. E. Stanley, *Nature* **376**, 46 (1995); P. Gopikrishnan, M. Meyer, L. A. N. Amaral, and H. E. Stanley, *European Physical Journal B* **3**, 139 (1998); P. Gopikrishnan, V. Plerou, L. A. N. Amaral, M. Meyer, and H. E. Stanley, *Physical Review E* **60**, 5305 (1999).
[7] R. F. Engle and A. J. Patton, *Quantitative Finance* **1**, 237 (2001).
[8] J. P. Fouque, G. Papanicolaou, and K. R. Sircar, *Derivatives in Financial Markets with Stochastic Volatility* (Cambridge University Press, Cambridge, 2000); *International Journal of Theoretical and Applied Finance*, **3**, 101 (2000).
[9] J. Hull and A. White, *Journal of Finance* **42**, 281 (1987); C. A. Ball and A. Roma, *Journal of Financial and Quantitative Analysis* **29**, 589 (1994); R. Schöbel and J. Zhu, *European Finance Review* **3**, 23 (1999).
[10] E. M. Stein and J. C. Stein, *Review of Financial Studies* **4**, 727 (1991).
[11] S. L. Heston, *Review of Financial Studies* **6**, 327 (1993).
[12] B. E. Baaquie, *Journal de Physique I (France)* **7**, 1733 (1997).
[13] R. Courant and D. Hilbert, *Methods of Mathematical Physics, vol. 2* (John Wiley & Sons, New York, 1962).
[14] R. P. Feynman and A. R. Hibbs, *Quantum Mechanics and Path Integrals* (McGraw-Hill, New York, 1965).
[15] L. S. Schulman, *Techniques and Application of Path Integration* (John Wiley & Sons, New York, 1981).
[16] H. Kleinert, *Path Integrals in Quantum Mechanics, Statistics, and Polymer Physics* (World Scientific, Singapore, 1995).
[17] E. Bennati, M. Rosa-Clot, and S. Taddei, *International Journal of Theoretical and Applied Finance* **2**, 381 (1999).

- [18] D. G. McMillan, *Applied Economics Letters* **8**, 605 (2001).
- [19] R. G. Tompkins, *Journal of Futures Markets* **21**, 43 (2001); Y.-N. Lin, N. Strong, and X. Xu, *Journal of Futures Markets* **21**, 197 (2001); G. Fiorentini, A. Leon, and G. Rubio, *Journal of Empirical Finance*, to be published.
- [20] C. W. Gardiner, *Handbook of Stochastic Methods for Physics, Chemistry, and the Natural Sciences* (Springer, Berlin, 1993).
- [21] C. M. Bender and S. A. Orszag, *Advanced Mathematical Methods for Scientists and Engineers* (Springer-Verlag, New York, 1999).
- [22] Y. Liu, P. Gopikrishnan, P. Cizeau, M. Meyer, C.-K. Peng, and H. E. Stanley, *Physical Review E* **60**, 1390 (1999).
- [23] I. S. Gradshteyn and I. R. Ryzhik, *Table of Integrals, Series, and Products* (Academic Press, New York, 1996), formula 3.914.
- [24] Yahoo Finance <http://finance.yahoo.com/>. To download data, type in the symbol box: “^DJI”, and then click on the link: “Download Spreadsheet”.
- [25] J. Masoliver and J. Perelló, preprints <http://lanl.arXiv.org/abs/cond-mat/0111334> and <http://lanl.arXiv.org/abs/cond-mat/0202203>.
- [26] J.-P. Bouchaud, A. Matacz, and M. Potters, *Physical Review Letters* **87**, 228701 (2001).
- [27] L. C. Miranda and R. Riera, *Physica A* **297**, 509 (2001).
- [28] R. Friedrich, J. Peinke and C. Renner, *Physical Review Letters* **84**, 5254 (2000); C. Renner, J. Peinke and R. Friedrich, *Physica A* **298**, 499 (2001).